U.S DEPARTMENT OF COMMERCE
NATIONAL OCEANIC AND ATMOSPHERIC ADMINISTRATION
NATIONAL WEATHER SERVICE
OFFICE OF SYSTEMS DEVELOPMENT
TECHNIQUES DEVELOPMENT LABORATORY

TDL OFFICE NOTE 93-3

HELICITY CHARACTERISTICS IN TORNADIC STORM ENVIRONMENTS FROM HOURLY WIND PROFILER DATA

K. Robert Morris and Ronald W. Kessler

May 1993

Helicity Characteristics in Tornadic Storm Environments From Hourly Wind Profiler Data

K. Robert Morris[1] and Ronald W. Kessler[1]

1. INTRODUCTION

The synoptic and thermodynamic patterns associated with severe thunderstorm activity are well known, and reliable techniques for forecasting such storms have been developed and are in use. However, methods for discriminating severe thunderstorm situations that are likely to produce strong tornadic activity from those which are not have been more elusive. Historically, the forecaster has relied on subjectively matching a given synoptic situation to one of a number of known synoptic patterns associated with tornado outbreaks (e.g., Miller 1972). Forecasters have become aware in recent years that the shear characteristics of the lower tropospheric winds bear a strong relationship to mesocyclone development and tornado activity associated with supercell thunderstorms.

Storm relative helicity has been shown to be a useful forecast tool for measuring the properties of the low-level wind shear associated with the development of strong tornadoes in a thunderstorm environment (Davies-Jones et al. 1990). Woodall (1990) has computed helicity from model forecast winds to forecast the tornadic potential for observed thunderstorms occurring within the model forecast periods. Analysis and display programs, such as the PC-based SHARP (Hart and Korotky, 1991) for rawinsonde data, and the HHPLOT program for wind profiler data on AFOS (Battel et al. 1993), have provided the forecaster with the means to display hodographs of low level winds and compute storm relative helicity for the observed wind profiles.

Previous studies on the relationship of helicity to tornado activity have been hampered by the lack of spatial and temporal continuity of the rawinsonde observations employed. It is recognized that high helicity values can and do occur with mesoscale features that cannot be routinely resolved by rawinsonde networks (Davies-Jones et al. 1990). Wind profiler data from the Wind Profiler Demonstration Network (WPDN) offer a unique opportunity to investigate applications of helicity to tornado forecasting.

Hourly profiler data from the dense network of profilers in Oklahoma have been analyzed in an attempt to answer some basic questions about the temporal and spatial variability of helicity. In particular, we wish to determine the characteristic scales of helicity in various synoptic situations, the relationship of helicity magnitude to tornadic activity and intensity, the possibility of developing accurate techniques of forecasting helicity, and whether there is important helicity information that can only be provided by a network of wind profilers.

2. HELICITY THEORY AND COMPUTATION

Simply stated, helicity is a measure of the horizontal component of vorticity (rotation about a horizontal axis) of air parcels in the inflow layer of a storm. Of more importance to tornado forecasting is the measure of this

---

[1]General Sciences Corporation, under contract to the Techniques Development Laboratory, Office of Systems Development, National Weather Service.

parameter in a storm relative sense. Storm relative helicity is the measure of this rotation relative to a moving storm. As air parcels in the inflow layer enter the updraft of a storm, the axis of rotation is tilted upward, effectively converting the horizontal vorticity of the inflow into the vertical component of vorticity in the updraft region. Positive (negative) helicities are associated with mesocyclones (mesoanticyclones). For the predominant veering wind profiles in the severe storm environment, the sense of the rotation and tilting contribute to the production of a mesocyclone circulation within the storm. Such mesocyclone circulations are typically observed within supercell thunderstorms.

The method used to compute helicity in this study follows from that described in Davies-Jones et al. (1990). Storm relative helicity for a layer of depth = h and for a given storm translation velocity $\boldsymbol{c} = (c_x, c_y)$ is computed from the relationship

$$H(c) = H(0) + \Delta v\, c_x - \Delta u\, c_y \qquad (1)$$

where $H(0)$, the ground relative helicity, and Δu and Δv, the components of the shear vector from 0 to h, are constants for a given wind profile. Values of h used in this study were 2 km and 3 km. No attempt is being made here to determine representative inflow depths for convective storms.

From Eq. 1 it can be shown that if the direction of the storm motion vector is the same as, or exactly opposite to, the direction of the shear vector from 0 to h, then the last two terms on the right sum to zero, and the storm relative helicity, $H(c)$, is the same as the ground relative helicity, $H(0)$. Equation 1 also shows that a storm moving to the right (left) of the shear vector receives a positive (negative) contribution to its storm relative helicity from the vertical shear of the winds within the layer. For a stationary storm ($c_x = c_y = 0$), the storm relative helicity is obviously the same as the ground relative helicity.

The ground relative helicity, $H(0)$, for the wind profile is computed from

$$H(0) = \sum_{n=0}^{N-1} (u_{n+1} v_n - u_n v_{n+1}) \qquad (2)$$

where (u_0, v_0) is the surface wind, (u_N, v_N) is the wind interpolated at height h, and (u_1, v_1), ..., (u_{N-1}, v_{N-1}) are the winds at intermediate levels between 0 and h. Note from Eq. 2 that, in the absence of any directional changes of the wind between 0 and h (i.e., a straight hodograph with or without speed shear), the ground relative helicity is equal to zero. The contribution to $H(0)$ of each pair of adjacent levels between 0 and h in Eq. 2 is positive (negative) for each layer where the wind veers (backs) with height.

The interest in helicity as a parameter for tornado forecasting is twofold. First, a requirement for high helicity in the storm inflow to support the development of mesocyclones (Brooks and Wilhelmson 1990), as well as for the stabilization of supercell structure in thunderstorms (Lilly 1986), has been

shown in modeling studies. In other words, there appears to exist some critical helicity threshold for the formation of tornadoes by way of the mesocyclone mechanism. Second, empirical studies have shown a relationship between the magnitude of helicity and the intensity of tornadic activity.

Based on a study of tornado proximity soundings for 28 tornado cases, Davies-Jones et al. (1990) have determined approximate ranges of helicities for three categories of tornado intensity: weak (F0,F1), strong (F2,F3), and violent (F4,F5) on the F0-F5 Fujita intensity scale. The three ranges correspond to 150-299 m^2/s^2 (weak), 300-449 m^2/s^2 (strong), and $\geq$ 450 m^2/s^2 (violent). As noted by these authors, the computation of storm relative helicity from Eqs. 1 and 2 is insensitive to the resolution of small-scale variations in the wind, and thus in a given environment, the helicity values and ranges derived from rawinsonde winds should be comparable in magnitude to those derived from profiler winds.

3. DATASETS AND PROCEDURES

The study area under consideration is defined by the area of coverage of RADAP-II data (McDonald and Saffle 1989) from the Oklahoma City (OKC) radar site. These data cover a circular area of 230 km (124 nautical mile) radius from the OKC radar, as shown in Fig. 1. This area encompasses four wind profiler sites [Vici (VCI), Lamont (LMN), Purcell (PRC), and Haskell (HKL)], and the Norman, Oklahoma (OUN) rawinsonde site. The four Oklahoma profilers are part of what is referred to as the inner network, a finer-spaced (approximately 200 km apart) network of profilers within the overall WPDN. The time period of the study covered the spring and early summer seasons from 21 March 1991 to 21 August 1991.

Primary datasets used in the study consist of:

1. RADAP-II 10-minute-interval data from the OKC radar
2. Hourly wind profiler and Profiler Surface Observing System (PSOS) data for the four stations of the WPDN inner network
3. Severe thunderstorm event reports from the NSSFC (National Severe Storms Forecast Center) logs
4. 0000 and 1200 UTC daily rawinsonde data from the OUN site
5. NGM (Nested Grid Model) gridded forecast winds at standard pressure levels (850-, 700-, 500-, 300-hPa), and at the 10-meter level, for the 6-, 12-, and 18-h projections from the 0000 and 1200 UTC model runs.

OKC RADAP-II data were used in the study for a number of purposes. Helicity as a forecast parameter has meaning only when thunderstorms are present or are expected to develop. Accordingly, edited RADAP-II convective cell data were used to identify dates and times of convective activity in the study area. Storm motion vectors (SMV's) computed from the edited cell data were used as a basis for computing storm relative helicity for individual storms. A method of estimating the expected storm motion is required in order to forecast expected values of storm relative helicity used to determine the tornadic potential prior to the onset of convection. SMV's are typically estimated

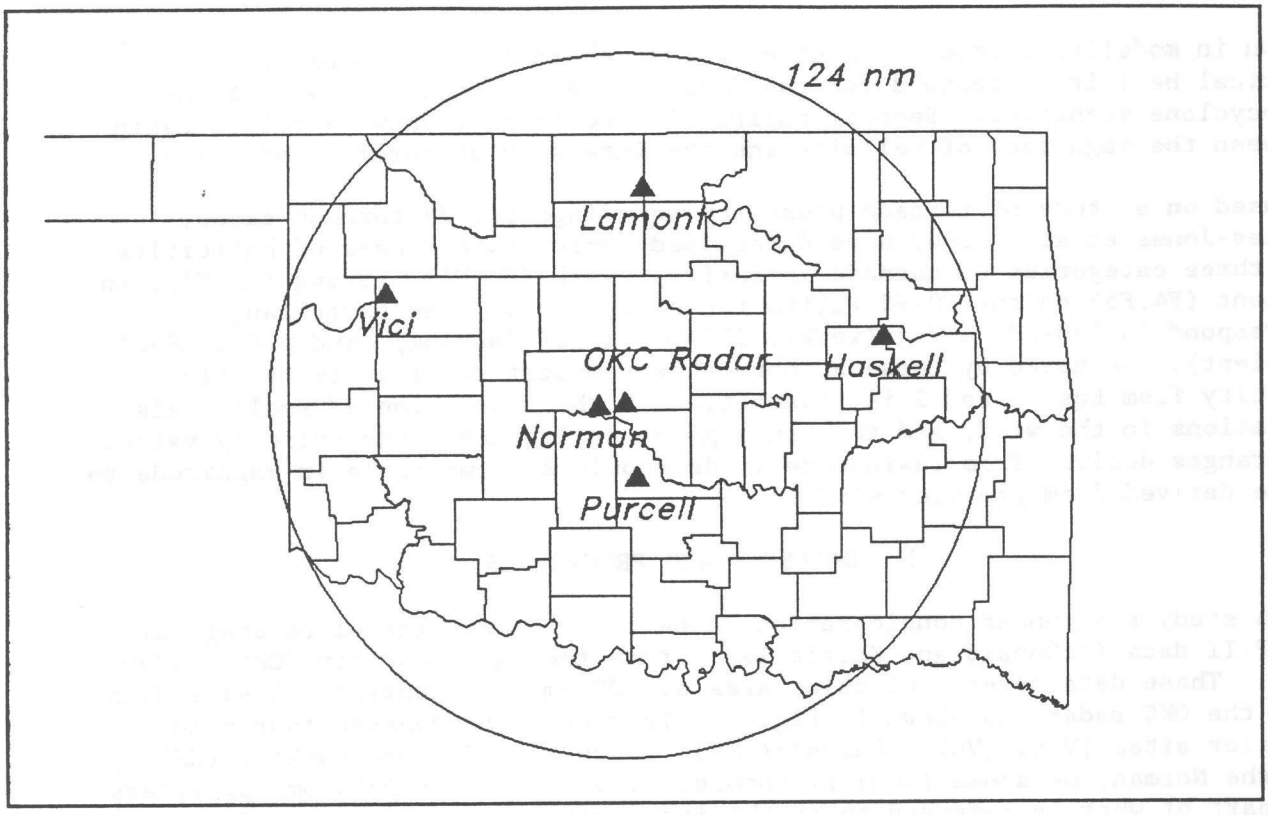

Figure 1. Study area inside the RADAP-II circular area of coverage for the OKC radar. Locations of the four profilers (Vici, Lamont, Purcell, and Haskell) and the Norman rawinsonde are shown.

from forecast or observed mid-tropospheric winds by selecting and modifying a single-level or mean layer wind that is closely related to the storm motion. The RADAP-II SMV's were compared to both observed and forecast winds to attempt to isolate various layers and levels in the atmosphere that can be used to estimate storm motion.

RADAP-II data processing followed the procedures described in Kitzmiller et al. (1992). A convective cell in the radar data is defined as a 28×28 km region containing a local maximum of ≥ 10 kg/m^2 in the VIL (Vertically Integrated Liquid water) field derived from the RADAP-II data. Each cell is centered on its local VIL maximum, and in some cases cells can overlap. Only those cells with a VIL value ≥ 10 kg/m^2 in 2 or more of the 4-km analysis grid boxes in the assigned region were considered. Severe weather events (tornado, hail ≥ 0.75 inch diameter, or wind gusts ≥ 50 kt) obtained from NSSFC storm logs were manually linked to cells. A given severe weather report was linked to only one cell. Event linkages to cells were restricted to times ranging from 20 minutes before to 10 minutes after the event time. A total of 1,351 convective cells are defined in the OKC RADAP-II data for the study period.

In this study, SMV's from the radar data were computed as mean cell center motions over the entire lifetime of the uniquely-identifiable convective cell

entities. This method of determining cell motion was selected to minimize the discretization error inherent in computing cell center displacements on the coarse 4-km grid. For the same reason, SMV's were computed for only those cells with lifetimes of 20 minutes or more. No attempt was made to separate the individual contributions of storm translation, propagation, and development to the overall cell motion.

Wind profiler data were processed into two sets of parameters. The first set of parameters consists of helicity coefficients A, B, and C computed for both the 0-2 km and 0-3 km inflow layers, where A, B, and C correspond, respectively, to the terms Δv, $-\Delta u$, and $H(0)$ in Eq. 1. As already noted, these terms are constants for a given wind profile and inflow depth. Winds at the tops of the defined inflow layers (2 km and 3 km) were linearly interpolated from the nearest good levels of profiler data above and below the layer tops. A profiler wind was assumed to be good unless it failed either the median or shear check in the profiler hub quality control procedure (Brewster 1989). No adjustment to the occasional low bias[2] to the wind speed in the first range gate was attempted.

Helicity coefficients were computed only for profiles where: (1) PSOS (surface) winds were present, (2) the first level of good winds in the profile was below 1 km AGL (above ground level), (3) at least one more good wind level was present between the first good level and 2 km AGL, and (4) at least one good wind level was present above 3 km AGL. If any of these conditions was not met, the wind profile was considered to be too incomplete to give a representative value of helicity.

The second set of parameters extracted from the profiler data consists of layer average u- and v-winds used for comparison to RADAP-II SMV's. The wind layers correspond to approximately the 850, 700, 500, 300, 850-700, 850-500, 850-300, 700-500, 700-300, and 500-300 hPa levels. A fixed range of heights encompassing multiple range gates of profiler data was assigned to each averaging layer, including single-pressure levels. Those profiler winds that failed either the median or shear check in the hub quality control were not used in the layer averaging. Winds used in the averaging were weighted by the depth of the layers between adjacent good wind levels.

Total wind speed and u- and v-wind components were averaged separately, and the averaged u- and v-wind components were used solely to derive an average wind direction for the layer. The layer average u- and v-winds were computed from the component-derived average wind direction and the directly-averaged total wind speed. This procedure was followed to eliminate the low bias in wind speed that can result from computing average wind speed directly from averaged components.

Helicity coefficients and layer-average winds were computed from the rawinsonde and NGM data in the same manner as for the profiler data, with minor exceptions. The gridded NGM data were horizontally interpolated to each of the four profiler locations before any other parameters were computed. Pressure and depth weighting were used to compute the layer wind averages

---

[2]Douglas Van De Kamp (1992), personal communication.

between pressure levels. No averaging or vertical interpolation was needed to extract the winds at the single-pressure levels.

4. CELL MOTION ESTIMATION

The single-level and layer-average winds (ambient winds) for the 10 levels defined in the study were compared to the RADAP-II SMV's to try to determine which wind level best estimates the measured storm motions. A simple scheme was used to match SMV's from cells, which occur at random times and locations, with winds from forecasts and observations, which have fixed locations and times. Cell positions and times were assigned the values taken at the mid-point of the cell lifetimes, as determined from the RADAP-II data. For each wind source, the station location and time (time only for the single site OUN rawinsonde winds) nearest to the cell midpoint were determined and assigned to the cell. For the NGM data, cells occurring between 0300 and 0900 UTC or between 1500 and 2100 UTC were assigned winds from both a 6-h and an 18-h projection with matching valid times from a pair of model runs 12 hours apart. The cell's RADAP-II SMV was compared to each layer and level wind for the assigned location and time(s).

In assigning cells to wind forecasts and observations, it was assumed that the wind data for all locations and times relating to the wind source were available. A complete set of motion comparison data for all cells was available from the NGM and OKC rawinsonde data, with the exception of a few missing levels and/or layer average winds in the rawinsonde data. However, due to missing wind profiler data, the expected hourly observation corresponding to the assigned hour and wind profiler location was not always available. If the nearest profiler hourly observation for a cell was missing, that cell was excluded from the comparison statistics for the profiler data. One cell with an obviously erroneous SMV speed was also excluded from all the comparisons.

Since wind is a vector variable, it is not possible to express differences or relationships between winds in a single statistic or value that suits all purposes. In this study, separate comparison statistics were computed for each wind source, each level or layer, and each component of the wind (direction and speed). For each of the 10 ambient wind levels or layers taken from the wind profile sources, the linear correlation coefficient, mean algebraic difference (ME), and mean absolute difference (MAE) between the wind speed and the cell SMV speeds were computed. For direction, only the mean algebraic difference and mean absolute difference between the wind and the SMV were computed. As computed here, a positive ME represents an overestimate of the measured RADAP-II SMV values by the ambient wind.

In the computations, the directional difference between the wind and the SMV was computed as values between -180° to +180°. In addition, for the ME calculations for wind direction, differences from 90° to 180° (-90° to -180°) were subtracted from 180 (-180) degrees to reduce large differences to the value range of from 90° to 0° (-90° to 0°). The purpose of this artificial reduction is that as the directional difference approaches +180° or -180°, a small change in the environmental or SMV wind direction can lead to a large change in the difference between the two (e.g., a directional difference of 179° is only two degrees away from a directional difference of -179°).

Results of the SMV comparisons to the ambient winds are shown in Tables 1 through 3. Statistics shown are the mean algebraic difference (ME), mean absolute difference (MAE), and linear correlation coefficient (CORR). Table 1 shows the comparison between SMV- and NGM-based wind speeds and directions for all cells for the 6- and 12-h projections. Positive ME values represent NGM values greater than the storm motion values. The speed ME's in Table 1 are mostly small and negative, except at 300 hPa where the ambient winds are significantly higher than the cell speeds. The linear correlation coefficients for the NGM wind speeds are low, explaining only about 30-40% of the variance of the measured cell motions. Directional ME's for all layers and levels are negative, indicating an overall tendency for the cells to move to the right of the forecast mid-level environmental winds. Mean absolute errors in using the NGM winds to predict cell motion direction are large at all levels, particularly for those including the 850-hPa winds.

Table 1. Speed and direction comparisons between RADAP-II storm motions and NGM-based single level and layer average winds. Comparisons are made to winds from the NGM projection (6- or 12-h) nearest to the midpoint of the cell's lifetime. Number of cases is 1,350 at each level and layer.

Level or Layer	Speed (m/s)			Direction (deg)	
	ME	MAE	CORR	ME	MAE
850	-1.77	4.77	.534	-26.62	67.78
700	-2.33	4.47	.609	-4.59	47.83
500	-.06	4.50	.587	-3.51	45.20
300	5.47	7.89	.522	-12.02	48.07
850-700	-2.07	4.47	.587	-18.24	55.53
700-500	-1.40	4.16	.629	-3.26	44.05
500-300	1.96	5.16	.573	-7.17	45.24
850-500	-1.69	4.15	.628	-9.57	46.50
700-300	.24	4.31	.613	-5.88	44.35
850-300	-.45	4.13	.629	-8.36	44.94

Table 2 shows the comparison between SMV- and rawinsonde-based wind speeds and directions for all cells. Overall, these results are similar to, but slightly poorer than, those for the NGM winds. As in the case for the NGM winds, there is no level or layer in the rawinsonde winds that stands out as obviously better for estimating cell motions. The 850- and 300-hPa levels and the 850-700 and 500-300 hPa layers are consistently worse than other levels in both sets.

Table 3 shows the comparison between SMV- and profiler-based wind speeds and directions for those cells where the nearest hourly wind profile was available. Note that the number of cases for this dataset is about half that of the NGM and rawinsonde datasets because of missing hourly profiler data. The

Table 2. Same as Table 1, except Norman rawinsonde winds from the sounding time nearest to the midpoint of the cell's lifetime. Number of cases at each level and layer ranged between 1244 and 1347.

Level or Layer	Speed (m/s)			Direction (deg)	
	ME	MAE	CORR	ME	MAE
850	-2.03	4.73	.383	-19.68	72.41
700	-1.42	4.45	.560	-3.52	50.55
500	2.09	5.00	.593	-9.23	48.88
300	6.16	8.05	.457	-11.06	56.75
850-700	-2.43	4.59	.538	-13.05	58.86
700-500	.75	4.57	.586	-1.55	44.47
500-300	3.64	5.91	.514	-10.14	47.97
850-500	-.73	4.26	.607	-5.58	45.84
700-300	1.89	4.72	.554	-6.97	44.57
850-300	.71	4.25	.574	-8.71	45.32

Table 3. Same as Table 1, except winds from the profiler and the hourly profile nearest in time and space to the midpoint of the cell's lifetime. No substitutions were made where the expected nearest profiler data were not available, which reduced the number of cases to 627 at each level and layer.

Level or Layer	Speed (m/s)			Direction (deg)	
	ME	MAE	CORR	ME	MAE
850	-1.90	4.70	.463	-16.26	63.16
700	-.92	4.27	.524	-3.93	49.73
500	1.27	4.93	.487	-8.46	49.92
300	5.34	7.23	.430	-16.26	55.58
850-700	-1.45	4.19	.529	-10.41	54.11
700-500	.33	4.42	.517	-4.82	48.06
500-300	3.45	5.49	.502	-12.57	51.37
850-500	-.33	4.07	.548	-7.23	48.87
700-300	2.08	4.70	.528	-10.36	48.46
850-300	1.35	4.32	.545	-11.02	48.37

statistics for the profiler winds are slightly poorer than for either the NGM or rawinsonde winds in terms of comparison to the radar cell motions, though the level and layer nearest 850 hPa showed some relative improvement in the profiler data.

The poor correlation between the SMV's and the ambient observed and forecast winds may be explained by a number of factors. The primary reason for the differences may be the large variability of the radar-derived cell motions to which the ambient winds are being compared. This variability in cell motion is due to many factors, including the combined effects of storm translation (the desired motion variable), propagation, and development; deviant storm motion; surface forcing; cell splitting and merging; and errors in the objective determination of cell motions by the automated technique. Other factors contributing to the differences include disturbances of the ambient winds in a convective environment (rawinsonde and profiler winds), and the differences in time (rawinsonde and model winds) and space (all wind sources) between the cells and the wind profiles. The relative smoothness of the NGM data, as compared to the observed winds from rawinsonde and profiler, may account for the slight improvement in the comparison statistics for the NGM winds.

Supercell thunderstorms are known to show deviant motion to the right (left) of the mean winds, which relates to the development of the storm's internal cyclonic (anticyclonic) rotation [e.g., Browning (1964)]. To investigate whether this deviant motion was contributing to the differences observed between the SMV's and the ambient winds, the comparison statistics for the profiler data were recomputed for only those cells which were associated with tornado and/or hail reports (those most likely to have supercell characteristics). These statistics are shown in Table 4.

Table 4. Same as Table 3, except only for those storm cells associated with tornado or hail reports. Total number of cases is 48 for each level and layer.

Level or Layer	Speed (m/s)			Direction (deg)	
	ME	MAE	CORR	ME	MAE
850	-0.40	4.77	.293	-28.93	48.75
700	2.52	4.48	.496	-22.50	43.71
500	5.88	7.08	.587	-15.92	44.38
300	9.98	10.98	.531	-20.75	43.29
850-700	.98	3.98	.452	-29.79	44.00
700-500	4.42	5.75	.576	-19.23	42.31
500-300	7.96	8.88	.582	-19.58	44.54
850-500	3.10	4.69	.567	-23.15	39.98
700-300	6.31	7.40	.575	-19.75	41.38
850-300	5.19	6.44	.578	-22.48	44.73

The larger negative ME's in direction shown in Table 4 as compared to those in Table 3 clearly show the tendency for cells associated with tornado or hail to move approximately 10-15 degrees more to the right of the ambient winds than all cells taken as a whole. The larger positive speed ME's in Table 4 compared to Table 3 indicate the slower motion of tornado and hail cells relative to the ambient winds and to all cells as a whole.

For Table 5, the statistics in Table 4 were recomputed by adjusting the profiler wind speed averages to 75% of their full value and adjusting the profiler wind direction averages 30 degrees to the right, based on the storm motion deviations from the 850-200 hPa winds as suggested by Maddox (1976). The adjustments to the profiler wind averages result in significant reductions in the speed and direction ME's, and lesser reductions in the MAE's. These findings support estimation of the SMV of tornadic storms by a wind that is 75% of the mean profile wind speed and 30° to the right of the mean profile direction for the 850-300 hPa layer, the study layer most closely matching the 850-200 hPa layer of Maddox. A smaller directional offset appears appropriate for mean layer winds not involving the 850 hPa level. The large variability between the SMV's and the observed winds means that for operational forecasting, forecasters are left with the challenges to be able to monitor or predict the actual degree of deviation of storm motion from the mean layer winds, and to establish under which situations these deviations are expected to occur.

Table 5. Same as Table 4, except profiler wind averages have been adjusted 30 degrees to the right and to 75% of their original speed prior to calculation of the statistics. Total number of cases is 48 at each level and layer.

Level or Layer	Speed (m/s)			Direction (deg)	
	ME	MAE	CORR	ME	MAE
850	-2.83	4.34	.293	-4.67	39.08
700	-.65	3.45	.496	1.33	36.58
500	1.87	4.17	.587	5.38	44.04
300	4.95	7.09	.531	2.88	42.17
850-700	-1.80	3.64	.452	-4.96	34.29
700-500	.78	3.44	.576	3.44	39.02
500-300	3.43	5.54	.582	2.63	45.38
850-500	-.21	3.06	.567	2.31	34.40
700-300	2.20	4.60	.575	3.83	41.21
850-300	1.35	3.98	.578	1.10	41.27

5. TORNADIC CASE STUDIES

Only a limited number of tornado days (six) were present in the 1991 dataset: five having multiple tornado events, and the remaining day having a single tornado. The wind profiler data for the nearest profiler to the storms were incomplete for a number of these cases. To achieve meaningful results from these data, it was necessary to undertake a case study approach to the investigation of profiler helicity applications. Time series of storm relative helicity from hourly profiler data were prepared to look at the temporal variability of helicity in the given synoptic situation. For storms occurring between profiler sites, a time series for each profiler believed to be representative of the storm environment was prepared to determine the spatial variability and continuity of helicity in relation to passing synoptic features. Unless otherwise stated, all helicity values mentioned or shown in the case study descriptions to follow are storm relative helicities for the 0-3 km layer.

A. 21-22 March 1991

A total of six tornadoes spawned from five separate storm cells were reported in the study area on March 21-22, in the area approximately 100-150 km east-southeast of the Purcell wind profiler. These storms occurred in association with a weakening front or dry line aligned NNE to SSW through central Oklahoma (Fig. 2), and were moving to the east-northeast at around 20 m/s. Profiler data were not available from the Purcell profiler, which had not yet been commissioned. The nearest available profiler data were from the Haskell profiler, 150-200 km north-northeast of the storms.

Individual time series of storm relative helicity computed with the observed SMV's for each of the five storm cells are shown in Fig. 3. Three of the storms occurred around 2300 UTC on the 21st, and were associated with tornadoes of F2, F2 and F3, and F1 intensities, respectively. The other two storms occurred around 0100 UTC on the 21st, with single tornadoes of F0 and F2 intensity. The wind profile was insufficiently complete to compute helicity at 0000 UTC on the 22nd. Storm relative helicities from the OUN rawinsonde at 0000 UTC on the 22nd were very low (-200 m^2/s^2 or less) and were wholly unrepresentative of the storm environment since the sounding was taken following the passage of the cold front.

Storm relative helicities around the times of the tornadoes are in the 150-200 m^2/s^2 range, relatively low for a multiple-tornado event with F2 and F3 intensity tornadoes. Due to the profiler's distance from the tornado events, it can not be assumed with a high level of confidence that the HKL profiler winds accurately represented the tornado environment for this case.

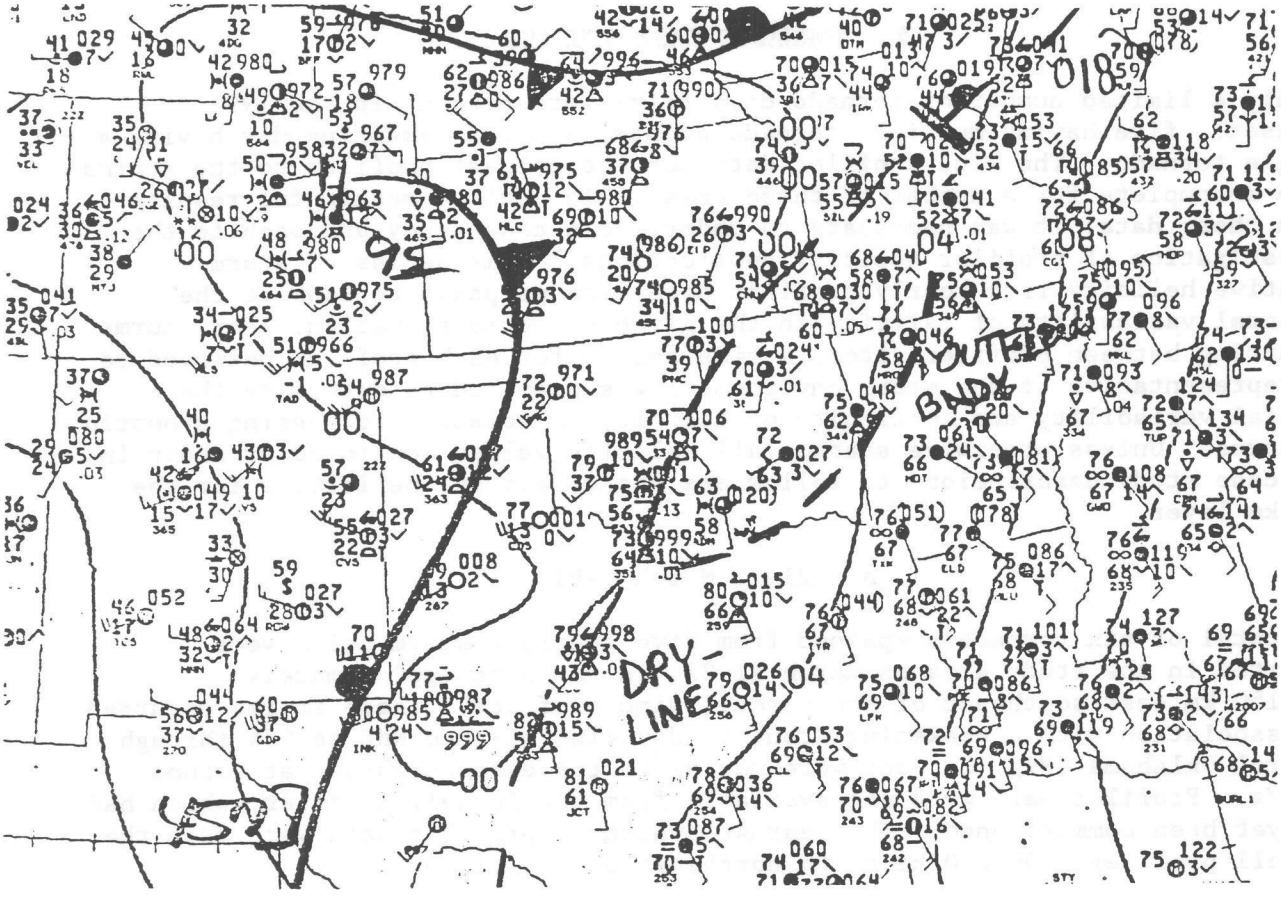

Figure 2. Surface analysis for 0000 UTC, 22 March 1991.

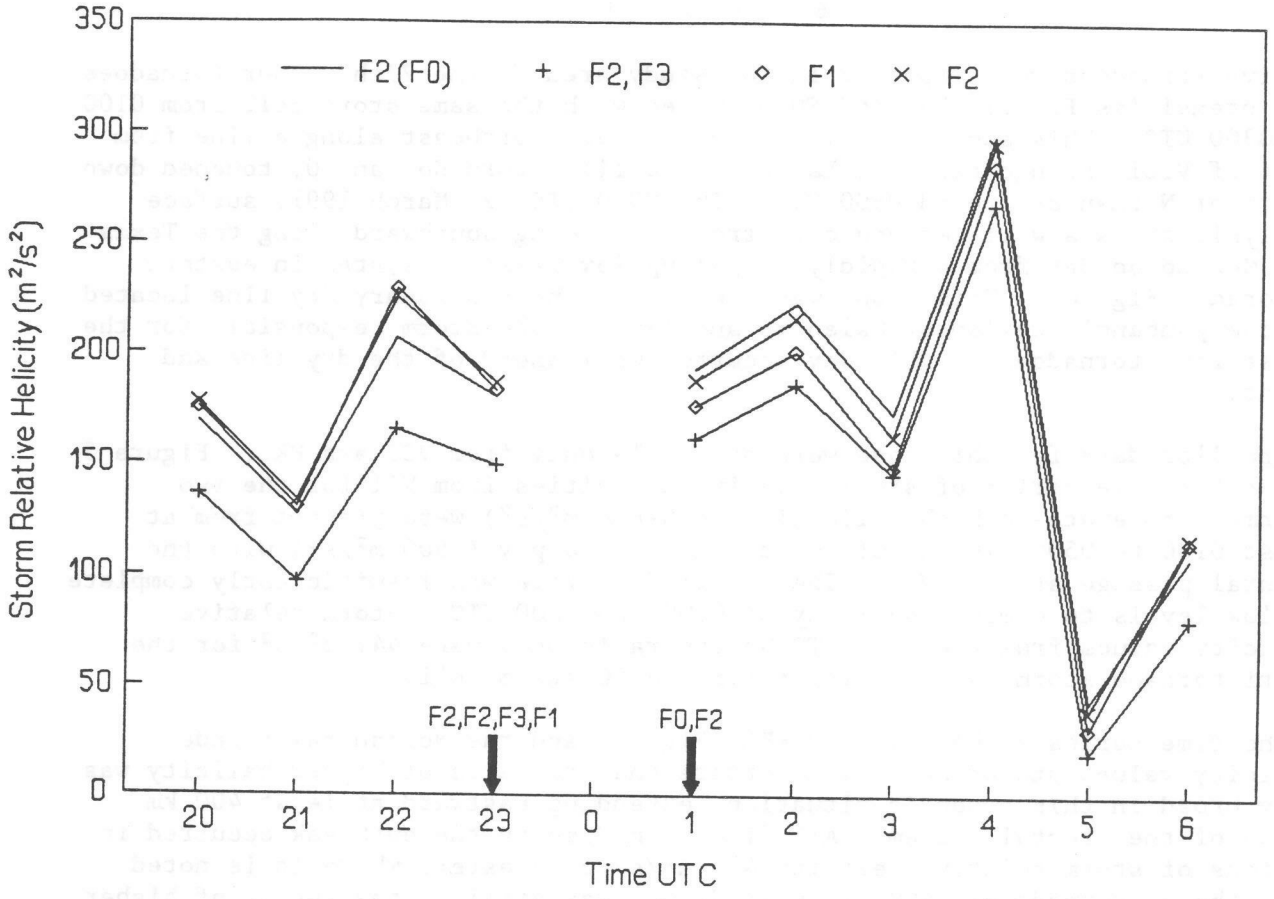

Figure 3. Time series of storm relative helicity from the Haskell, Oklahoma, wind profiler for five tornadic storms on 21-22 March 1991. Times of occurrence of the tornadoes are indicated by arrows along the time axis of the plot. Line labeled F2(F0) in the legend indicates two separate tornadic storms at 2300 and 0100 UTC with the same storm motion, and resultantly the same values of storm relative helicity. Helicities were not computed at 0000 UTC due to missing critical levels in the profiler data.

B. 27 March 1991

Five tornadoes were reported in the study area on the 27th. Four tornadoes of intensities F0, F2, F3, and F0 occurred with the same storm cell from 0100 to 0300 UTC. This storm cell moved to the east-northeast along a line from east of Vici through north of Lamont. The fifth tornado, an F0, touched down north of Norman at around 0600 UTC. The 0000 UTC, 27 March 1991, surface analysis shows a well-defined cold front extending southward along the Texas-New Mexico border from a rapidly deepening low pressure system in eastern Colorado (Fig. 4). This front was overtaking the stationary dry line located in the panhandle region of Oklahoma and Texas. The storm responsible for the first four tornadoes on this day occurred well ahead of the dry line and front.

Profiler data for this case were available only from VCI and HKL. Figure 5 shows the time series of storm relative helicities from VCI for the two storms. Moderate-to-high helicities (400-600 m^2/s^2) were present from at least 0100 to 0500 UTC at VCI, dropping off sharply (-500 m^2/s^2) with the frontal passage at 0600 UTC. The VCI wind profile was insufficiently complete at low levels to compute helicity at 0000 and 0600 UTC. Storm relative helicity values from the 0000 UTC Norman rawinsonde were 441 m^2/s^2 for the multi-tornado storm, and 483 m^2/s^2 for the F0 storm cell.

The time series of helicity at HKL (Fig. 6) and the Norman rawinsonde helicity values stated above demonstrate that the area of higher helicity was very broad in this synoptic situation, extending eastward at least 400 km ahead of the frontal system. All five tornadoes in the outbreak occurred in regions of storm relative helicity 400 m^2/s^2 or greater, where it is noted that the F0 tornado at 0600 UTC near Norman was still in the region of higher helicity ahead of the front. If it can be assumed that the VCI helicity time series before 0100 UTC showed a pattern similar to that at HKL 2-3 hours later, then the time scale over which moderate to high helicity can occur for such a weather pattern appears to be on the order of 6 hours or more.

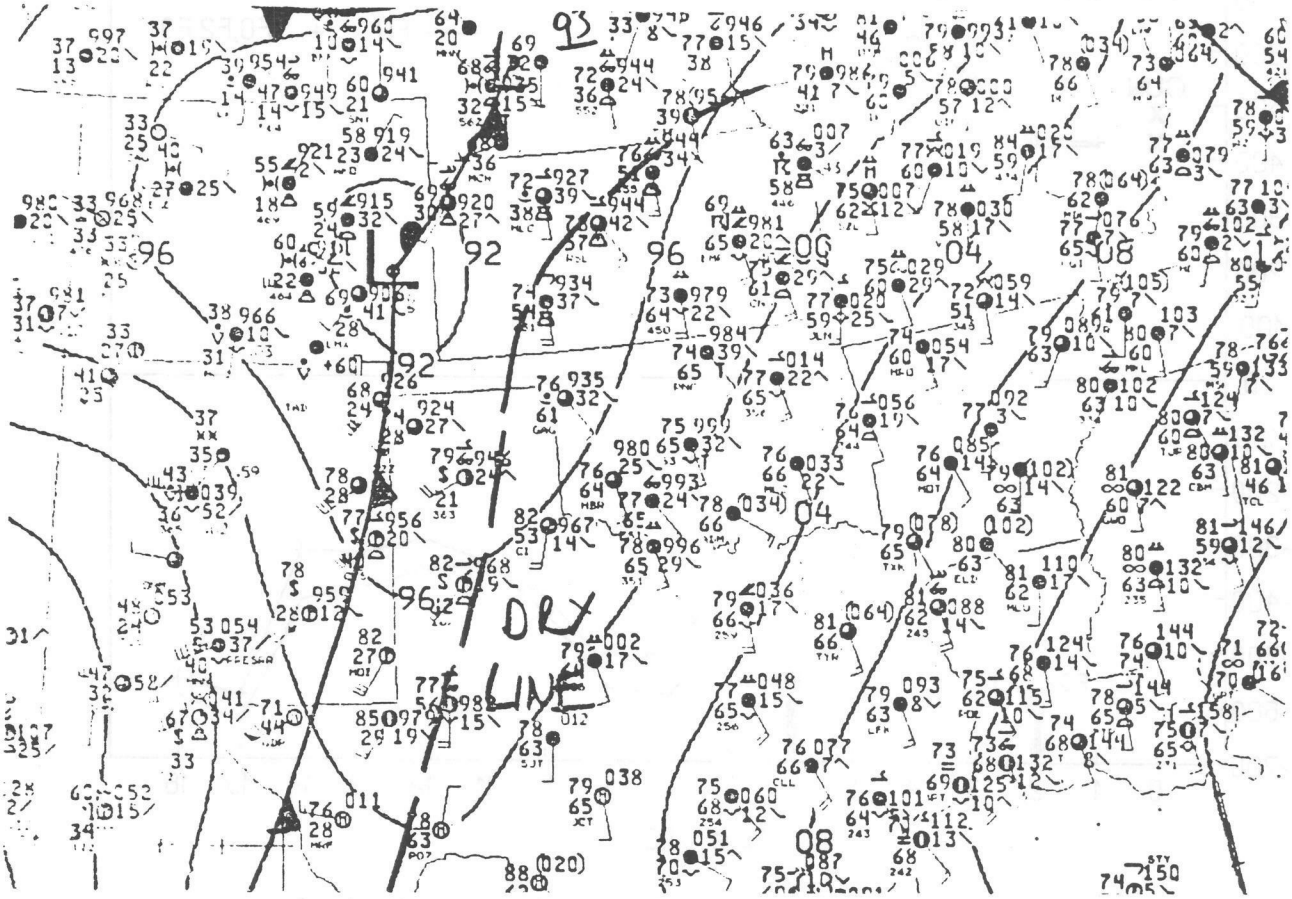

Figure 4. Surface analysis for 0000 UTC, 27 March 1991.

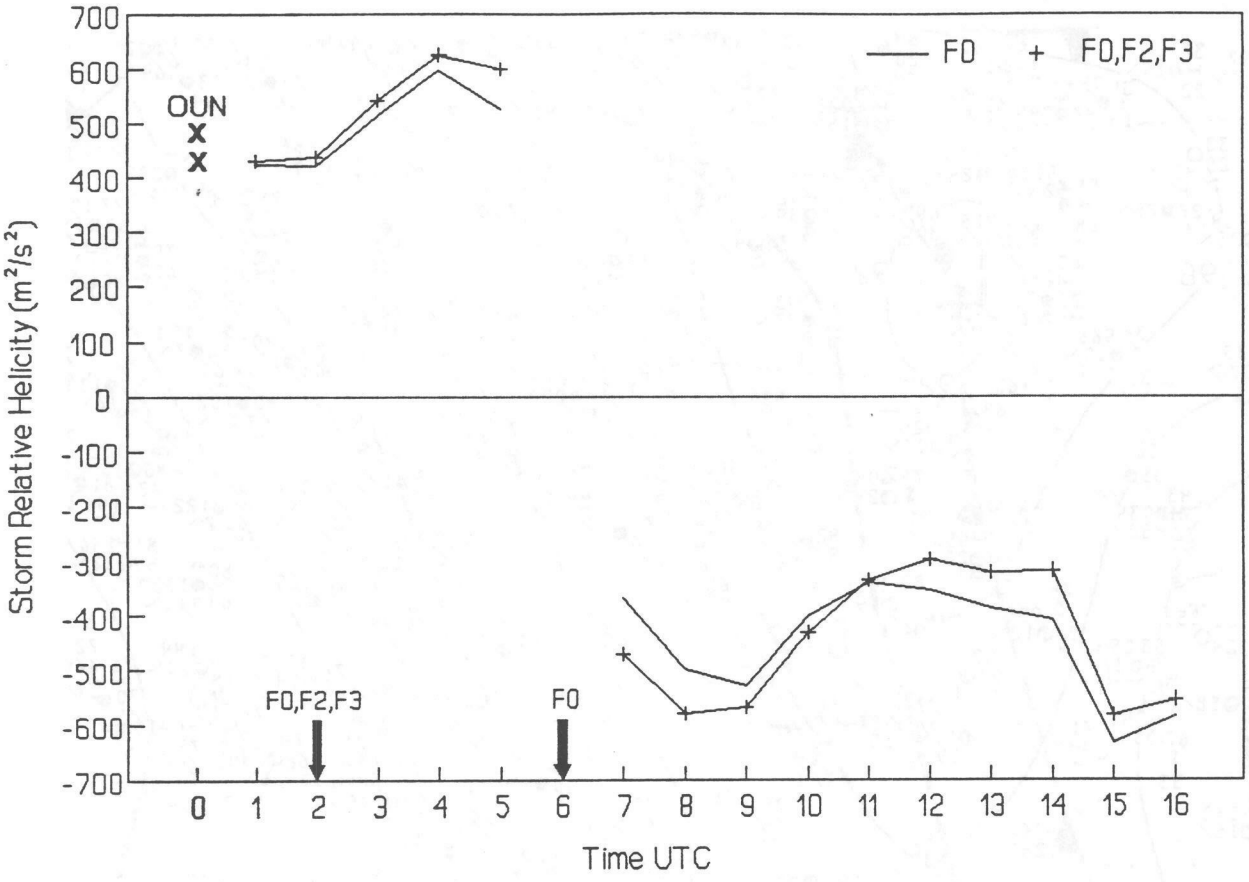

Figure 5. Time series of storm relative helicity from the Vici, Oklahoma, wind profiler for two tornadic storms on 27 March 1991. Times of occurrence of the tornadoes are indicated by arrows along the time axis of the plot. Helicities were not computed at 0000 and 0600 UTC due to missing critical levels in the profiler data. The heavy X's indicate OUN rawinsonde helicities.

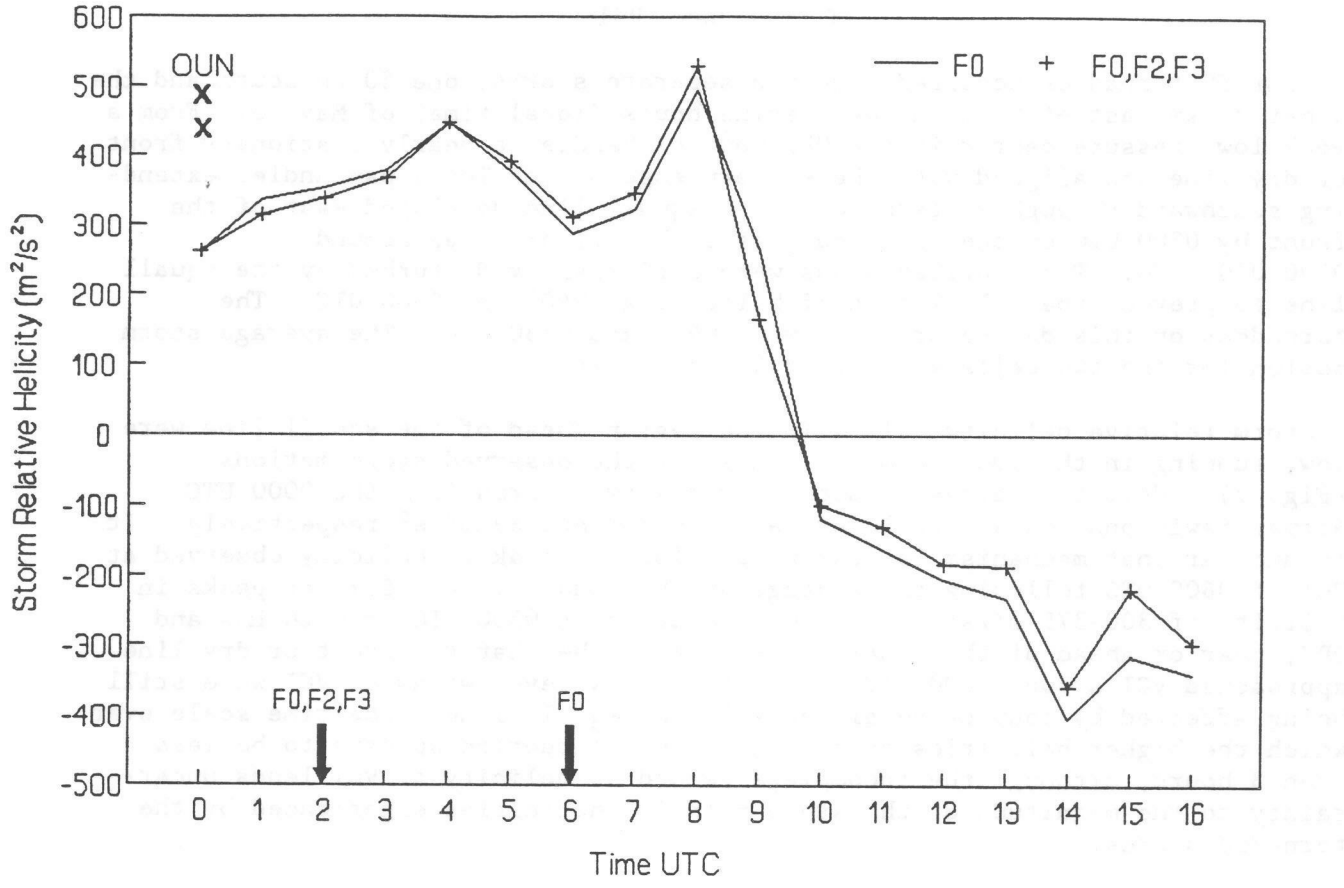

Figure 6. Time series of storm relative helicity from the Haskell, Oklahoma, wind profiler for two tornadic storms on 27 March 1991. Times of occurrence of the tornadoes are indicated by arrows along the time axis of the plot. The heavy X's indicate OUN rawinsonde helicities.

C. 16 May 1991

Four F0 tornadoes occurred with two separate storms, one 80 km south and the other 30 km east of Vici in the evening hours (local time) of May 15. From a weak low pressure center in the Oklahoma panhandle, a nearly stationary front or dry line was aligned with the eastern edge of the Texas panhandle, extending southward through western Texas. A squall line developed east of the front by 0300 UTC on the 16th and passed the VCI profiler around 0400-0500 UTC. The profiler winds were sufficiently disturbed by the squall line to prevent the calculation of helicity at 0400 and 0500 UTC. The tornadoes on this day occurred between 0430 and 0530 UTC. The average storm motion for the two cells was from 245° at 15 m/s.

Storm relative helicity values in the region ahead of the squall line were low, running in the 100-200 m^2/s^2 range for the observed storm motions (Fig. 7). Helicity values computed for the two storms from the 0000 UTC Norman rawinsonde data were lower, at 19 m^2/s^2 and 89 m^2/s^2 respectively. It is unclear what mechanism is responsible for the peak in helicity observed at VCI at 0600 UTC following the passage of the squall line. Similar peaks in helicity of 300-375 m^2/s^2 (not shown) occurred at 0500 UTC at both LMN and PRC, near or ahead of the squall line. It may be that the front or dry line approached VCI around 0600 UTC, or that the low level winds at VCI were still being affected by convective elements in the squall line. The time scale over which the higher helicities developed in this situation appears to be less than 3 hours, although the incomplete record of helicity at VCI lends uncertainty to the magnitude of the storm relative helicities experienced by the tornadic storms.

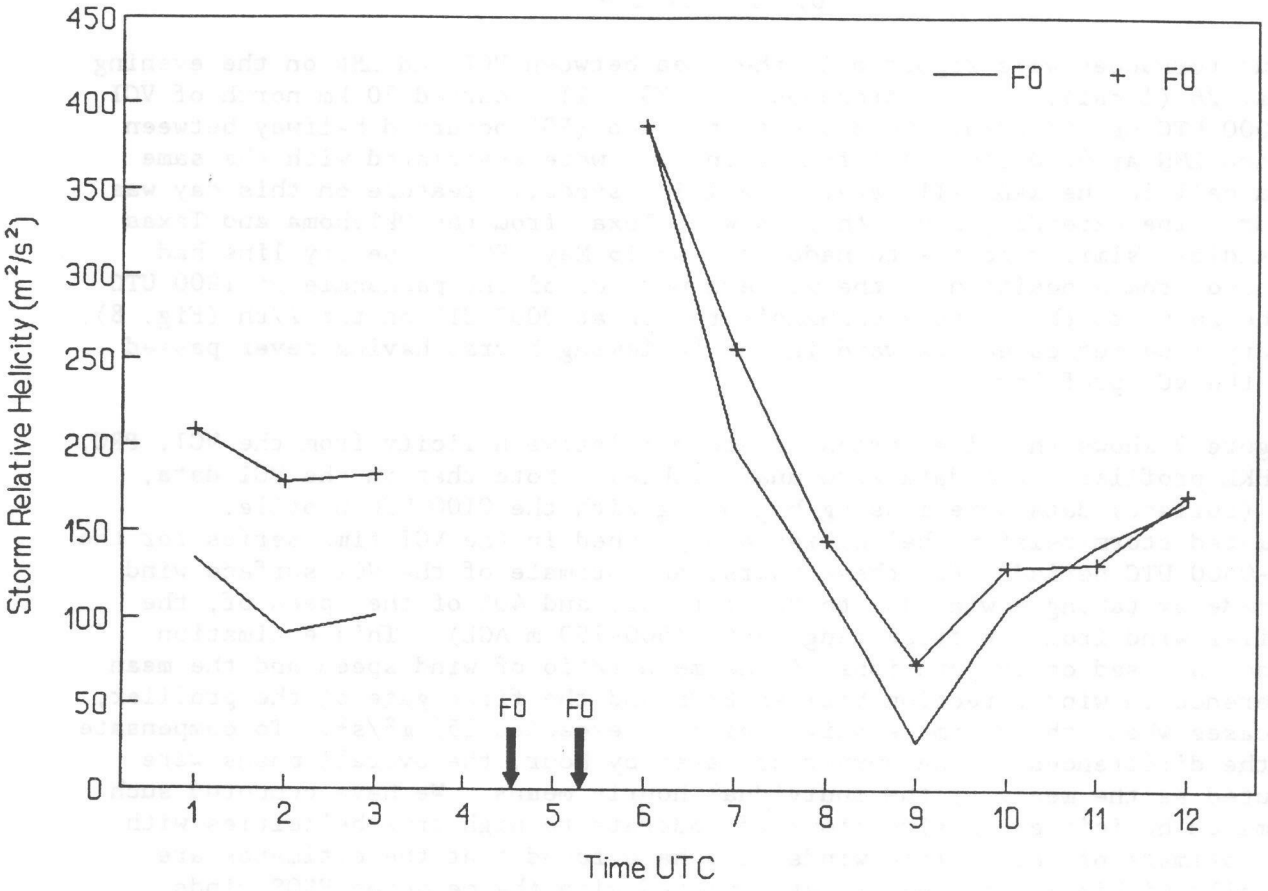

Figure 7. Time series of storm relative helicity from the Vici, Oklahoma, wind profiler for two tornadic storms on 16 May 1991. Times of occurrence of the tornadoes are indicated by arrows along the time axis of the plot. Helicities were not computed at 0400 and 0500 UTC due to missing critical levels in the profiler data.

D. 27 May 1991

Four tornadoes were reported in the area between VCI and LMN on the evening of May 26 (local). Three tornadoes (F1, F3, F1) occurred 30 km north of VCI at 0000 UTC on the 27th, and a fourth tornado (F0) occurred halfway between VCI and LMN at 0200 UTC. All four tornadoes were associated with the same storm cell in the RADAP-II data. The major synoptic feature on this day was the dry line extending south through west Texas from the Oklahoma and Texas panhandles, similar to the tornado case on 16 May 1991. The dry line had advanced from a position in the western portion of the panhandle at 1800 UTC on the 26th, to the eastern panhandle region at 0000 UTC on the 27th (Fig. 8). The dry line retreated westward in the following hours, having never passed over the VCI profiler.

Figure 9 shows the time series of storm relative helicity from the VCI, PRC, and HKL profilers (LMN data were unavailable). Note that in the VCI data, PSOS (surface) data were missing beginning with the 0100 UTC profile. Estimated storm-relative helicities are graphed in the VCI time series for the 0100-0600 UTC period. For these hours, an estimate of the VCI surface wind was made by taking a wind 30° to the left of, and 40% of the speed of, the profiler wind from the first range gate (500-750 m AGL). This estimation method is based on computations of the mean ratio of wind speed and the mean difference in wind direction between PSOS and the first gate of the profiler, for cases where the storm relative helicity exceeded 150 m^2/s^2. To compensate for the differences in the number of cases by hour, the overall means were computed as the means of the individual hourly means. We have computed such estimated helicities in situations of moderate to high true helicities with this estimate of the surface winds, and have found that the estimates are generally within 10% of the values computed with the measured PSOS winds.

A rapid rise in storm relative helicity occurred at VCI between 2200 and 0000 UTC with the approach of the dry line. Winds at VCI in the 0-3 km layer showed increases in speed and in the amount of veering accompanying the helicity increases after 2200 UTC. A 50-kt low level jet was evident in the VCI profiler data at 500-1000 m AGL from 0400-1200 UTC.

Comparison of the Fig. 9 time series at VCI with those at PRC and HKL reveals the small spatial and time scales of helicity associated with the wandering dryline feature. Helicity at VCI increased from 120 to at least 420 m^2/s^2 in a 2-h period when the dry line approached to within about 100 km of the profiler. In contrast, helicity at PRC and HKL showed only the gradual increases during the evening hours that typically occur with diminished convective mixing, and did not appear to be influenced by the dry line 200 km or more to the west. The storm relative helicity derived from the 0000 UTC, 27 May, Norman rawinsonde was also low, with a value of 95 m^2/s^2. The first three tornadoes in this case occurred near VCI during the sharp rise in helicity when the storm relative values were over 400 m^2/s^2. The weaker F0 tornado at 0200 UTC occurred 50 km farther east of dry line than the first three, most likely in an area of slightly lower helicity.

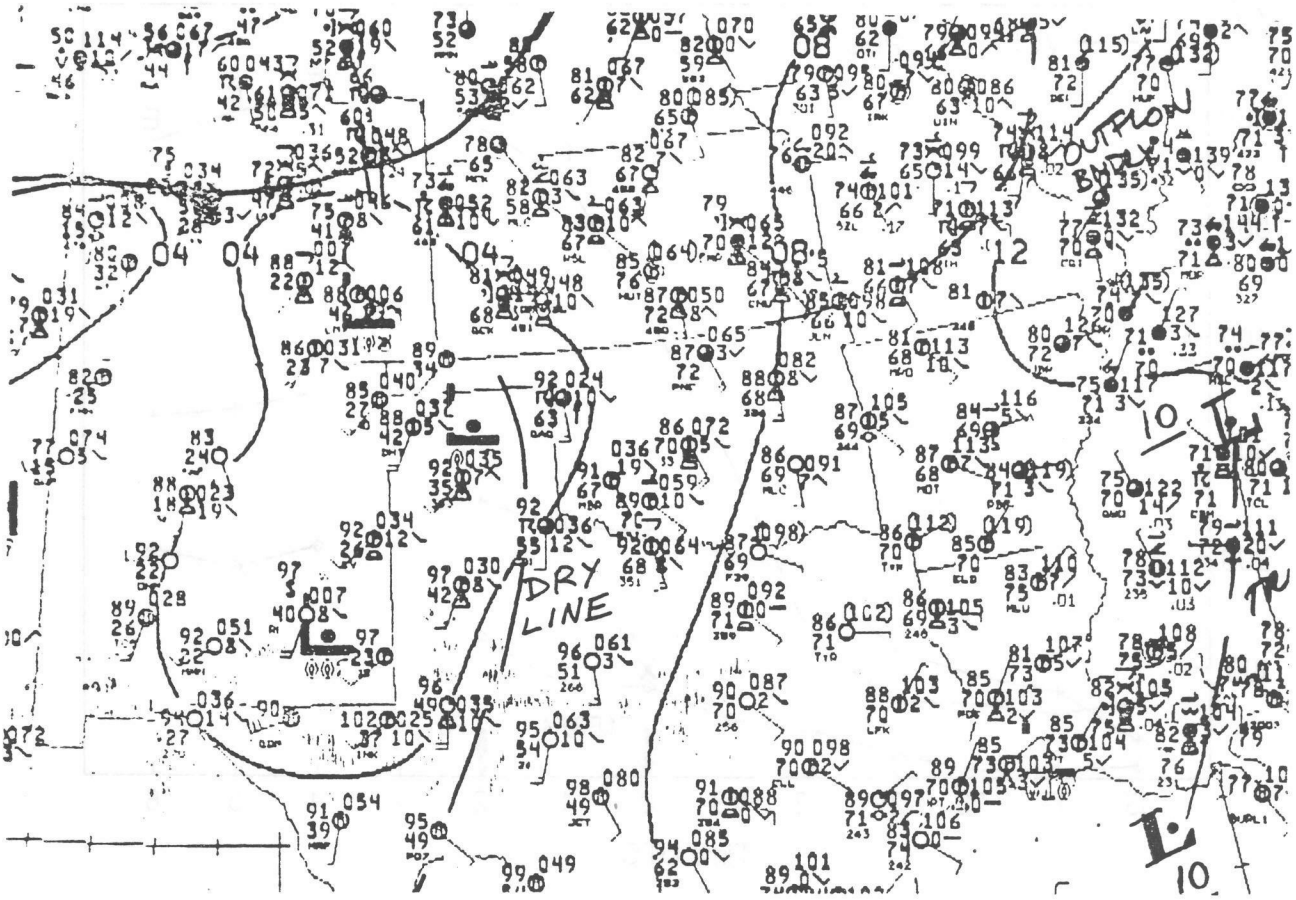

Figure 8. Surface analysis for 0000 UTC, 27 May 1991.

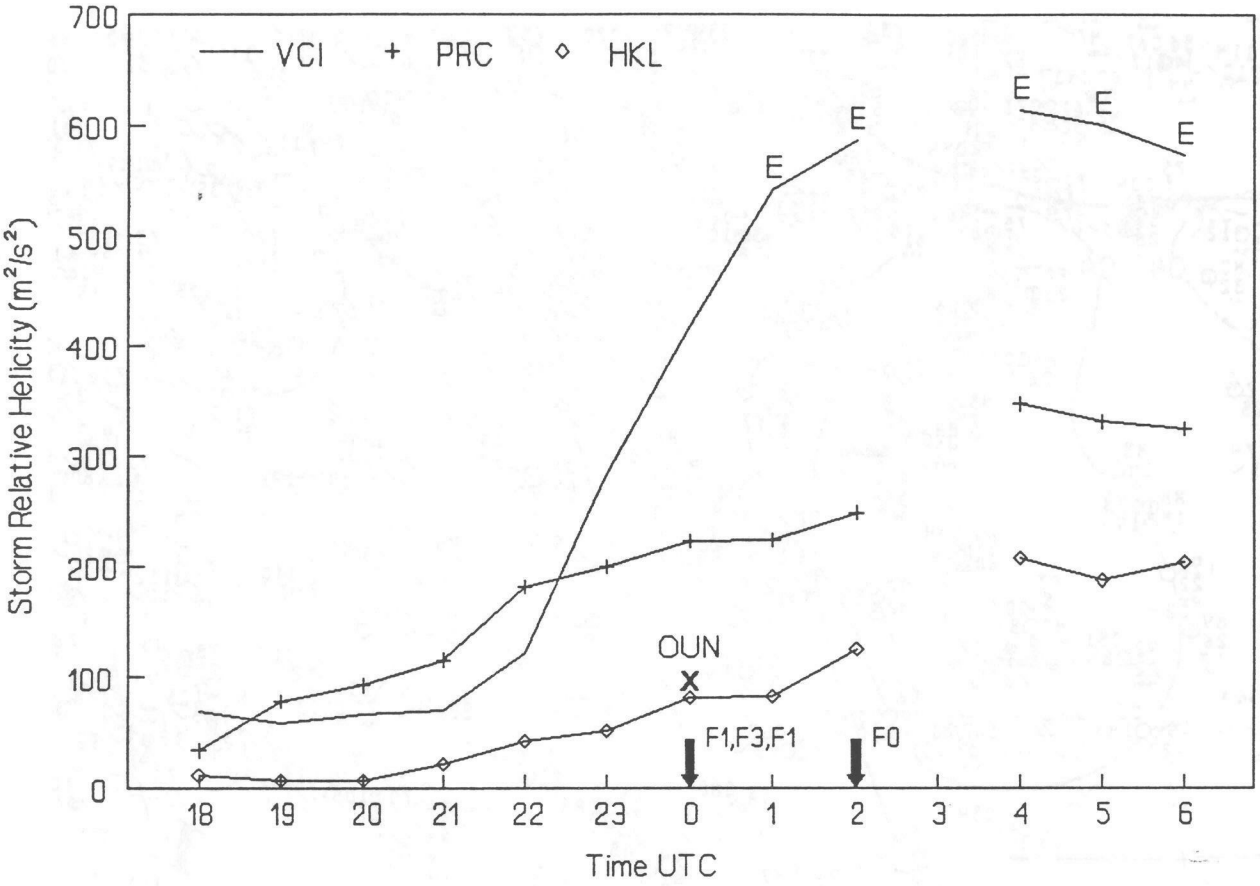

Figure 9. Time series of storm relative helicity from the Vici (VCI), Purcell (PRC), and Haskell (HKL), Oklahoma, wind profilers for a tornadic storm on 26-27 May 1991. The heavy X indicates the storm relative helicity value based on the 0000 UTC rawinsonde from Norman, Oklahoma (OUN). Times of occurrence of the tornadoes are indicated by arrows along the time axis of the plot. Helicities at VCI after 0000 UTC (labeled E) were computed with estimated surface winds to substitute for missing PSOS wind data (see text).

E. 5 June 1991

Severe thunderstorms developed during the morning of June 5, triggered by decaying outflows from slow-moving overnight storms in Kansas and northern Oklahoma. Storms spread south across Oklahoma along the expanding outflow boundary, and two brief F0 tornadoes occurred around 1800 UTC (noon CST) in southern Oklahoma, about 150 km south of HKL. This case differs from those already described in that there was no organized, synoptic-scale feature influencing the winds in the study area.

Helicities at the time of the tornadoes were low, as seen in Fig. 10. At 1200 UTC, prior to the passage of the outflow boundary, helicities at the Norman (OUN) rawinsonde and the HKL and PRC profilers were low at around 210, 130, and 90 m^2/s^2, respectively. Helicity showed only slight increases to 150-170 m^2/s^2 during the hours prior to the outflow passage at the profilers, and dropped below 100 m^2/s^2 following passage of the outflow boundary at HKL (1400 UTC) and PRC (1800 UTC). The low helicity and weak tornadoes on this day are consistent with the type of activity expected with low-shear, gust front thunderstorms, where the mechanisms for tornado formation differ from those associated with mesocyclone development in high helicity environments.

F. 13 July 1991

A weak front trailing west-southwestward into a pressure trough lay across north-central Oklahoma between Lamont and Norman at 0000 UTC on 13 July, with weak winds of 25 knots or less throughout the lower and middle levels of the atmosphere. Showers and thunderstorms were widespread along either side of the surface feature between 0000 and 0300 UTC. A single F0 tornado occurred around 0200 UTC between Norman and Lamont in an environment of very low helicity. The helicity value computed from the 0000 UTC Norman sounding was 53 m^2/s^2, while the hourly helicity values at LMN between 0000 and 0500 UTC were all less than 40 m^2/s^2. No time series of helicity is shown for this marginal case since the helicity values are low and nearly constant with time.

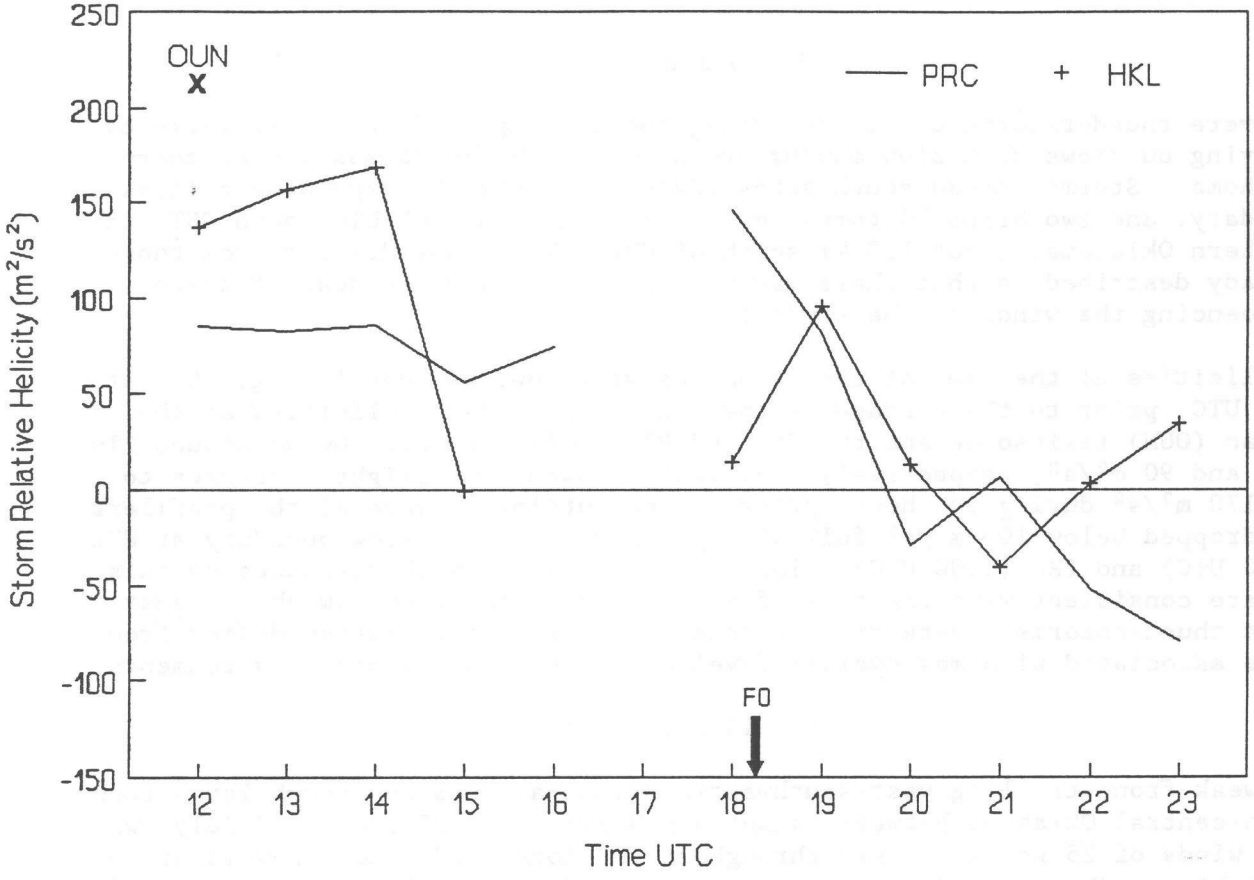

Figure 10. Time series of storm relative helicity from the Purcell (PRC), and Haskell (HKL), Oklahoma, wind profilers for a tornadic storm on 5 June 1991. The heavy X indicates the storm relative helicity value based on the 1200 UTC rawinsonde from Norman, Oklahoma (OUN). Time of occurrence of the tornado is indicated by arrow along the time axis of the plot. Helicities were not computed at HKL at 1600 UTC due to missing critical levels in the profiler data, and profiler data at both PRC and HKL were unavailable at 1700 UTC.

G. SUMMARY OF CASE STUDIES

The relationship between storm relative helicity and tornado intensity for the tornadic case studies in 1991 is shown in Table 6. The event units in this table are individual tornadic storm cells identified in the RADAP-II data, where the maximum tornado intensity is assigned to the cell for cases of multiple-tornado cells. For cases where the time and space matchings between the profiler data and the tornado event are not close, the helicity values represent a subjective selection of the profiler and the hour most representative of the tornado environment, chosen from the available data for the case. Although the number of cases are few, some limited conclusions can be drawn from the case study data.

Table 6 shows that except for F0 tornadic cells, a relationship between increasing tornado intensity and increasing storm relative helicity appears to exist. F0 tornadic cells occurred over all ranges of helicity. However, except for the two F0 cells on 16 May (where the helicity values are uncertain), all the F0 cells with helicities over 150 m^2/s^2 occurred in outbreaks also having tornadic cells of greater intensity. Significantly, no tornadic cells of F1 or greater intensity occurred in environments of low helicity (<150 m^2/s^2). Thus, while weak tornadoes may routinely occur in environments of moderate to high helicity values, it appears that the probability of occurrence of F1 or stronger tornadoes is very low in situations of low helicity.

Table 6. Contingency table of 1991 Oklahoma storm-relative helicities from profilers categorized by tornado intensity. Events are counted by cell, taking only the maximum tornado intensity for a cell.

Helicity (m^2/s^2)	Tornado Intensity				Total Events
	F0	F1	F2	F3	
≤150	2	0	0	0	2
151-300	2	1	2	1	6
301-450	2	0	0	1	3
>450	1	0	1	1	3
Total	7	1	3	3	14

Helicities computed from NGM forecast data (not shown) showed little skill in forecasting tornado activity. NGM derived helicities were probably unrepresentative of the storm environment due to the poor low-level vertical resolution of the model forecast data.

The synoptic pattern in which severe thunderstorms occur determines the time and space scales characteristic of the helicity, and hence, the lead time that can be expected for observing and forecasting high helicity situations. The case study storm of 27 March 1991 shows that ahead of a strong frontal system associated with a deep low pressure center, broad (~400 km wide) areas of high helicity can be present for 6 hours or more prior to passage of the front. At the opposite extreme, the dryline case of 27 May shows how helicity values can be concentrated within 100 km of a dynamically weak synoptic feature. The case on 27 May demonstrated how, when the dry line advances, helicity at a point ahead of the dry line can rise sharply in a period of 2 hours from background values (<150 m^2/s^2) to values supporting moderate to strong tornado activity (>400 m^2/s^2).

6. RELATED RESULTS

In the course of analyzing helicity from hourly profiler data for 1991 Oklahoma convective storms, several general results important to the operational use of helicity in tornado forecasting were uncovered. First, a diurnal variation in profiler-derived helicity was observed on most days in the study period. Figure 11 shows the mean hourly storm-relative helicity averaged over all dates and all four profilers in the 1991 Oklahoma dataset. For Fig. 11, storm motions in the hourly helicity computations were estimated by a wind 20 degrees to the right and 75% of the speed of the 700-500 hPa layer average wind in the hourly profiles. The estimation method is based on the SMV estimation results in Tables 4 and 5.

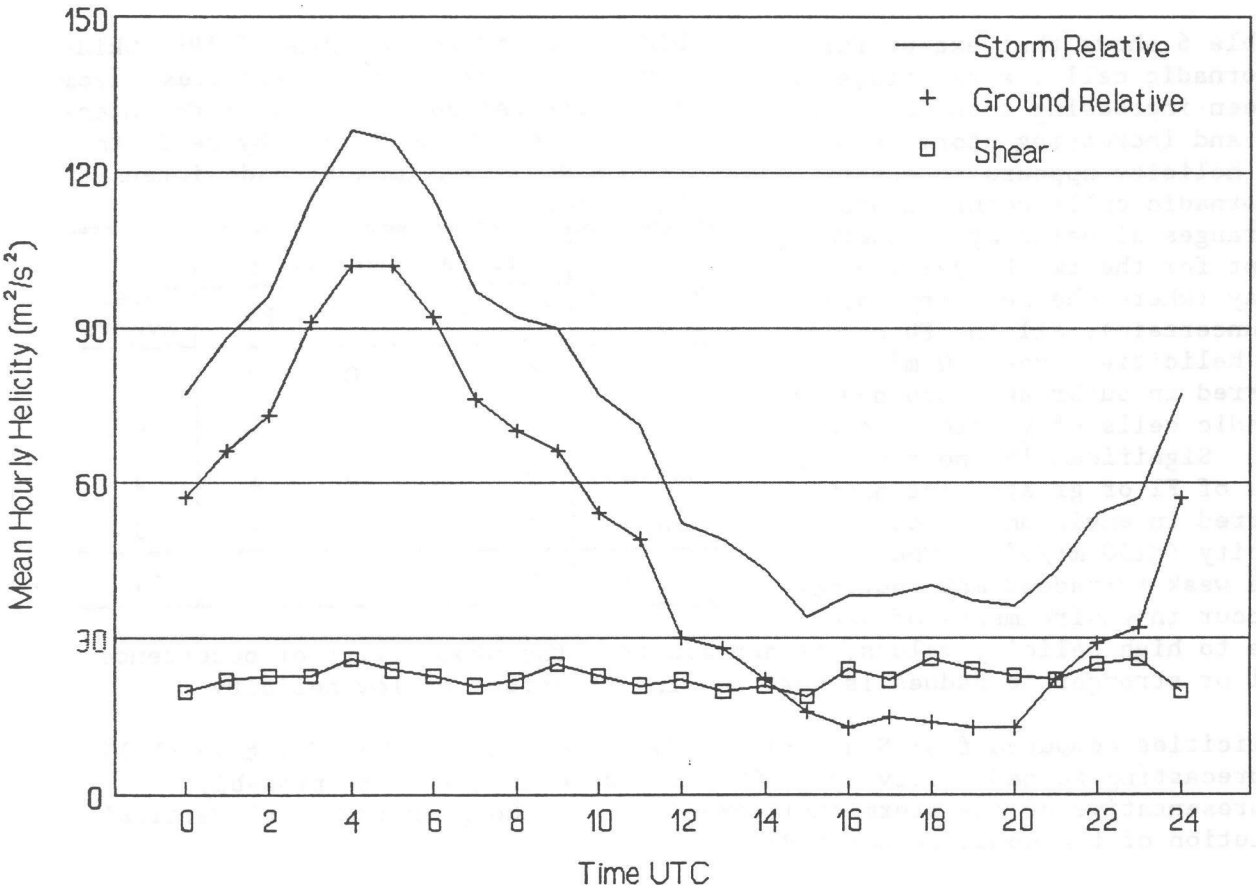

Figure 11. Mean storm-relative helicity, ground relative helicity, and shear helicity values by hour (UTC) for the four Oklahoma profilers, for all convective days in the study area from 21 March to 21 August 1991.

On average, an increase in helicity begins to develop in the afternoon near 3 p.m. local time (2100 UTC for Oklahoma) and reaches a maximum around 10 p.m. local time (0400 UTC). This increase is observed only in the ground relative helicity term ($H(0)$ in Eq. 1), as shown in Fig. 11. The average contribution of the shear term to the storm relative helicity is nearly constant at around 24 m^2/s^2. Thus it appears that the increase in helicity is due to increased veering and more monotonic speed increases with height of the low level winds from the late afternoon hours into the evening. Such changes in the low level

winds would be expected during this time, as deep convective mixing diminishes and frictional forces in the lower levels of the atmosphere assume a relatively greater role in shaping the wind profile. It remains to be investigated whether the eveningtime increases in helicity are a precursor of, or are related to, the development of a low level jet in the following hours.

Figure 12 shows the percent of hourly storm-relative helicities from Fig. 11 that exceed each of three critical thresholds (150, 300, and 450 m^2/s^2). It is clear that the diurnal variation of helicity values operates over all ranges of helicity, and that the probability of exceeding a selected threshold is greatest in the hours from 10 p.m. to 4 a.m. local time (0200 to 0900 UTC). For comparison, the number of Oklahoma tornadoes by hour in the intensity ranges F0 to F1 and F2 to F5 are shown in Fig. 13. The data in Fig. 13 are for the months March through August, for the four years 1988 to 1991. For this small sample, the diurnal maximum in helicity is not reflected in the number of tornadoes occurring during the hours of the helicity maximum. However, the peak hour for the F2 to F5 tornadoes (0200 UTC) is nearer to the time of the average helicity maximum than is the peak hour for F0 and F1 tornadoes (2300 UTC).

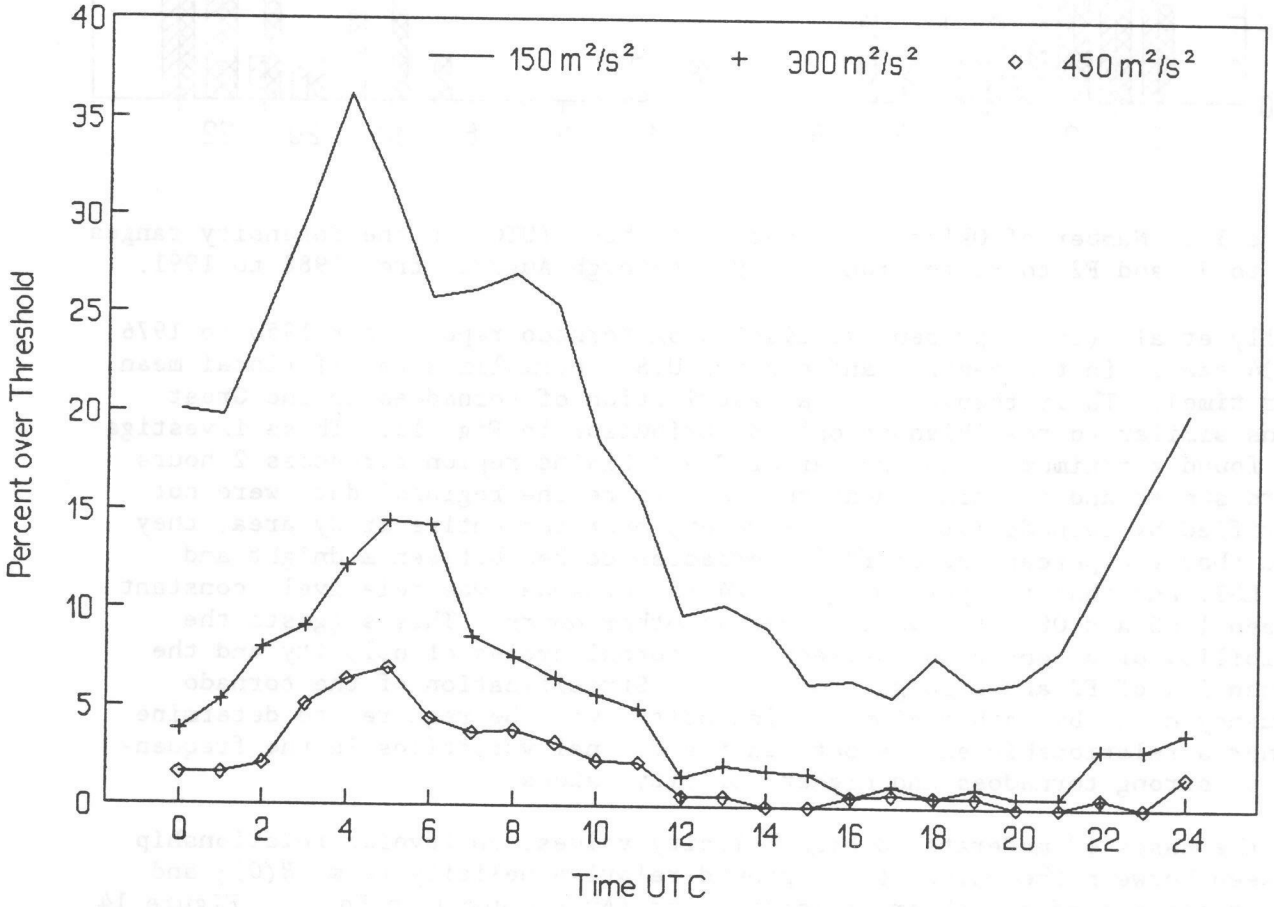

Figure 12. Percent of hourly storm-relative helicities that exceed each of three critical thresholds (150, 300, and 450 m^2/s^2). Helicity is computed for the same data and in the same manner as in Fig. 11.

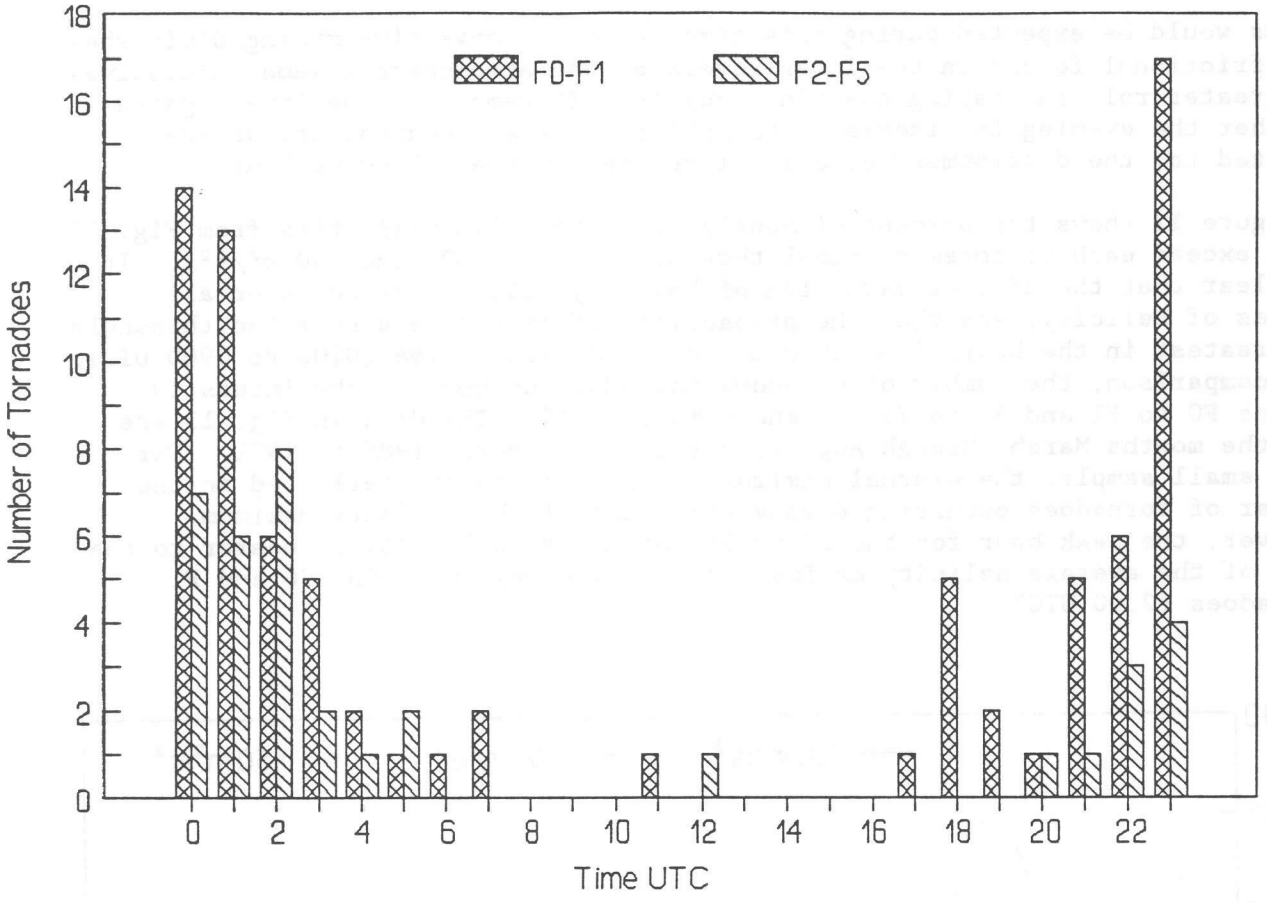

Figure 13. Number of Oklahoma tornadoes by hour (UTC) in the intensity ranges F0 to F1 and F2 to F5 for months March through August, from 1988 to 1991.

Kelly et al. (1978) present statistics on tornado reports for 1950 to 1976 for 24 states in the central and eastern U.S., normalized to LST (local mean solar time). Their results show a distribution of tornadoes in the Great Plains similar to the Oklahoma-only distribution in Fig. 13. These investigators found a maximum in the number of Great Plains region tornadoes 2 hours before sunset and a minimum near sunrise, where the regional data were not stratified by tornado intensity. However, over the entire study area, they found that the percentage of F2-F3 tornadoes peaked between midnight and 0600 LST, and that the percentage of F4-F5 tornadoes was relatively constant between 1400 and 0000 LST while lower at other hours. This suggests the possibility of a connection between the diurnal cycles of helicity and the frequencies of F2 and stronger tornadoes. Stratification of the tornado frequency data, by both region and intensity, will be required to determine whether a relationship exists between the diurnal variations in the frequencies of strong tornadoes and higher helicity values.

In the cases of moderate to high helicity values, an inverse relationship was seen between the value of the ground-relative helicity term [$H(0)$] and that of the sum of the shear helicity terms ($\Delta v\, c_x - \Delta u\, c_y$) in Eq. 1. Figure 14 shows an example from the HKL profiler for 21-22 March 1991 where, as the storm relative helicity climbs from 200 to 300 m^2/s^2 between 2200 and 0400 UTC, the ground relative helicity increases from -20 to 250 m^2/s^2, while

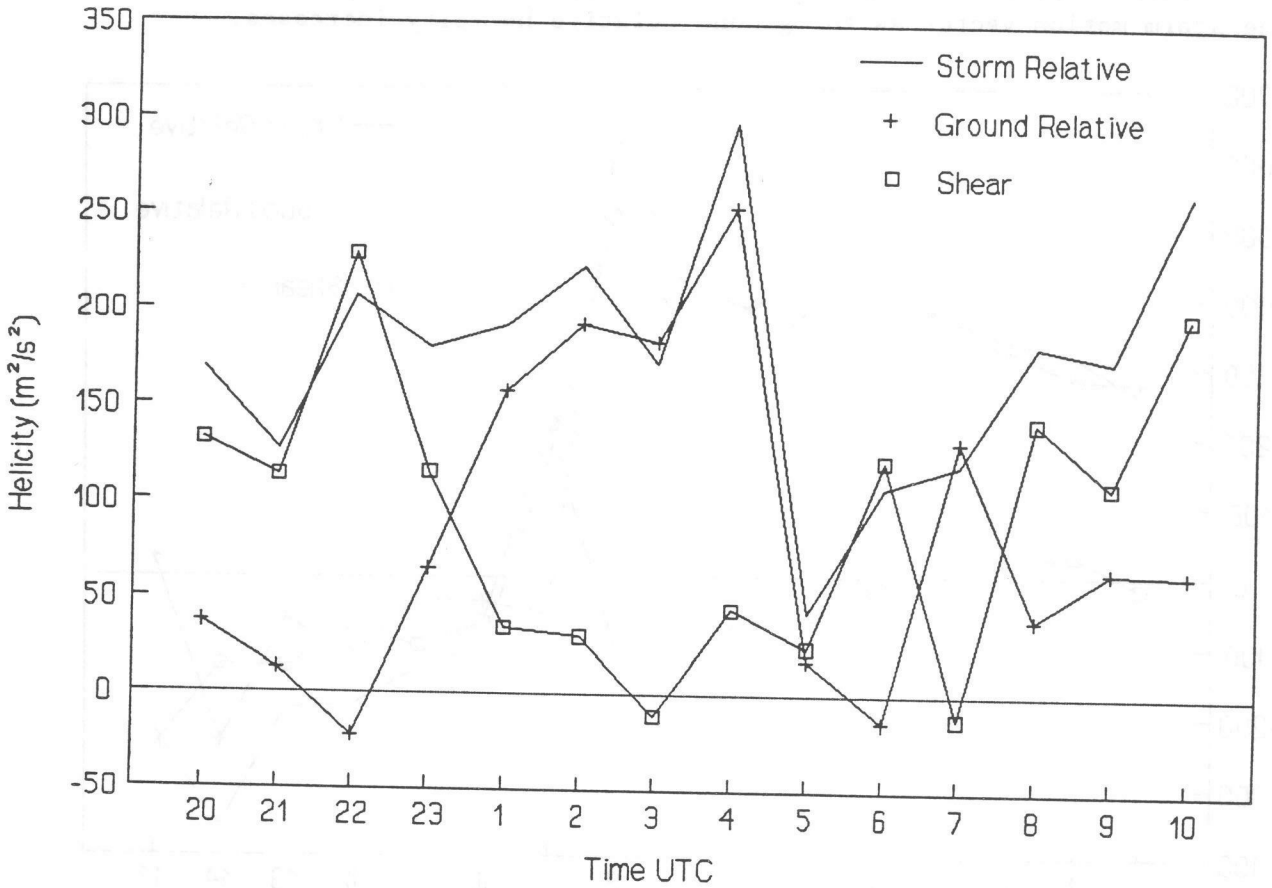

Figure 14. Time series of total storm-relative helicity, ground relative helicity, and shear helicity values by hour (UTC) for the Haskell, Oklahoma, wind profiler for an F2 tornadic storm on 21-22 March 1991.

the shear helicity decreases from 230 to around 50 m^2/s^2. Figure 15 shows the storm-relative, ground-relative, and shear helicity from the HKL profiler data based on the F3 tornadic cell motion on 27 March 1991. During the period of moderate to high helicity between 0000 and 0800 UTC, the ground relative helicity starts off at a moderate value (250 m^2/s^2), and increases to a peak of 500 m^2/s^2, while the shear helicity starts near zero and then decreases to about -100 m^2/s^2. In the dryline case at VCI on 26 May, the change in storm relative helicity up to 0000 UTC (Fig. 8) was due almost entirely to changes in the ground relative helicity, while the shear term oscillated within values of ± 30 m^2/s^2.

These results imply that the influence of the storm motion in the computation of storm relative helicity is most critical in cases where the ground relative helicity is less than 200-300 m^2/s^2. For ground relative helicity above 300 m^2/s^2, the storm motion and shear vectors were seen to line up directionally, and as a result the shear appears to have little effect on value of the storm relative helicity. Additionally, shear magnitudes were observed to remain relatively constant compared to the changes in the ground relative helicity. Thus, in the absence of any extreme anomalies between the storm motion and shear directions (40 degrees or more), any significant increases in helicity in these situations will be mostly due to the ground

relative term. The storm relative helicity becomes relatively less sensitive to the storm motion vector as the ground relative helicity increases.

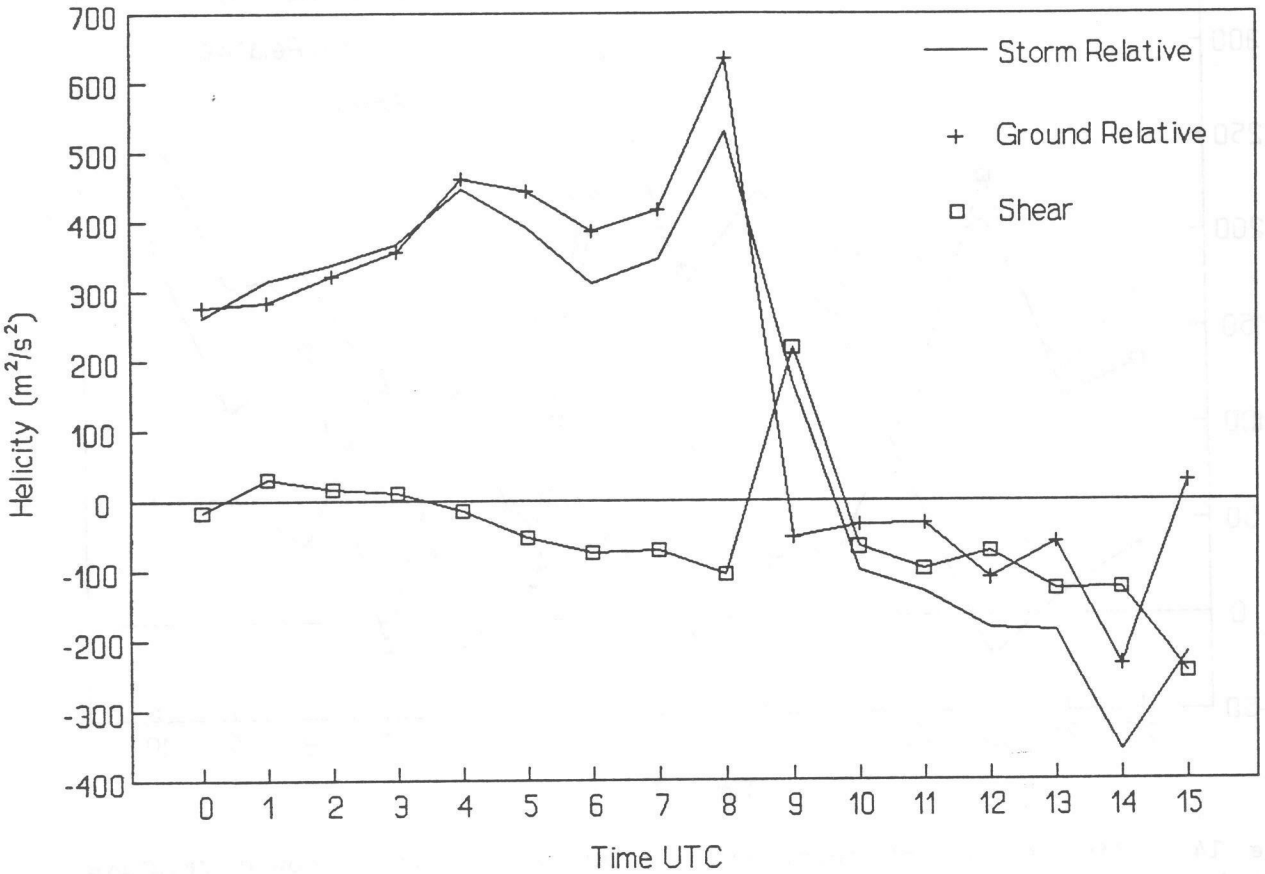

Figure 15. Time series of total storm-relative helicity, ground relative helicity, and shear helicity values by hour (UTC) for the Haskell, Oklahoma, wind profiler for an F3 tornadic storm on 27 March 1991.

7. SUMMARY AND CONCLUSIONS

Hourly wind profiler data from the dense inner network of profilers in Oklahoma have revealed new information about the temporal and spatial variability of storm relative helicity in the convective environment. In cases of strong, large-scale synoptic features such as a major cyclonic system, areas of high helicity extended out to 400 km ahead of the cold frontal passage and persisted for 6 hours or more in time. For the case of a sub-synoptic scale feature (the Texas-Oklahoma dry line), high helicity values were confined to within 100 km of the moist side of the dry line, and increased over a period of 2 hours from background values (<150 m^2/s^2) to values capable of supporting moderate to strong tornado activity (>400 m^2/s^2).

Observed tornado intensities were related to the magnitude of the storm relative helicity derived from profiler winds. All tornadoes on the case study days that occurred in environments of low helicity (<150 m^2/s^2) were weak (F0) tornadoes. All tornadoes of F1 or greater intensity occurred in environments of medium to high helicity (≥ 150 m^2/s^2). The small number of

cases and the incompleteness of the 1991 profiler data did not allow the more specific empirical relationship between tornado intensity and helicity magnitude presented by Davies-Jones et al. (1990) to be verified.

Storm motion vectors estimated from layer-average winds showed a poor correlation to cell motions measured from RADAP-II data. This poor correlation may be due to multiple factors including: 1) natural variability of storm motions; 2) low spatial resolution of the RADAP-II VIL analysis; 3) problems associated with objective determination of storm cell motions from the RADAP-II data; and 4) NGM, profiler, and rawinsonde layer average winds that are unrepresentative of the storm motions. The layer average winds from the NGM and from rawinsonde were slightly better at estimating storm motion than those from the profiler.

Although the correlations were still poor, the storms associated with tornado and hail reports showed a significant deviant motion to the right of, and slower than, the profiler layer average winds. Cell motions estimated by a wind that is 75% of the mean profile wind speed and 30 degrees to the right of the mean profile direction for a selected layer result in significant reductions in the speed and direction ME's, and lesser reductions in the mean absolute differences. Of the wind levels and layers used in the study, no single-level or layer-average wind stood out as the best estimator of storm motions.

Cases where storm relative helicity exceeds 300 m^2/s^2 demonstrated a reduced sensitivity to the influence of storm motion. Two factors contribute to this insensitivity. First, the observed storm motion directions were seen to approach the 0-3 km shear vector directions when helicity values increased to values approaching 300 m^2/s^2, reducing the contribution of shear to the storm relative helicity. Second, the variation of the ground relative helicity exceeded the variability in the magnitude of the 0-3 km shear. These results indicate that the forecaster must be most concerned with establishing a good value of expected storm motion for cases where helicity is in the marginal range for tornado activity (i.e., around 150 m^2/s^2).

A distinct eveningtime maximum in helicity was evident in the Oklahoma profiler data on many days in the study period. On average, a helicity maximum occurs around 10 p.m. local time and is due exclusively to increases in the ground-relative helicity component. The average difference between the daily minimum and maximum helicity values is ~95 m^2/s^2. The apparent similarity between the daily helicity cycle and the hourly frequency of F2 and stronger tornadoes found by Kelly et al. (1978) remains to be investigated.

8. ACKNOWLEDGEMENTS

The authors are grateful to Messrs. Luther A. Carroll, David H. Kitzmiller, and Wayne E. McGovern of the Techniques Development Laboratory for reviewing the draft of this paper, and for their many helpful comments and suggestions. This work was performed as part of the National Weather Service's Wind Profiler Assessment Program led by the Office of Meteorology. Monetary support was provided by the Forecast Systems Laboratory of NOAA's Environmental Research Laboratories.

9. REFERENCES

Battel, G. F., M. A. Leaphart, J. T. Moeller, and M. A. Petrie, 1993: AFOS profiler software system. NOAA Techniques Development Laboratory Computer Program NWS TDL CP 93- , National Weather Service, NOAA, U.S. Department of Commerce, 188 pp. (In draft)

Brewster, K. A., 1989: Quality control of wind profiler data. Wind Profiler Training Manual Number Two, Program for Regional Observing and Forecasting Services, Environmental Research Laboratories, NOAA, U.S. Department of Commerce, 39 pp.

Brooks and Wilhelmson, 1990: The effect of low-level hodograph curvature on supercell structure. Preprints 16th Conference on Severe Local Storms, Banff, Amer. Meteor. Soc., 34-39.

Browning, K. A., 1964: Airflow and precipitation trajectories within severe local storms which travel to the right of the winds. J. Atmos. Sci., 21, 634-639.

Davies-Jones, R., D. Burgess, and M. Foster, 1990: Test of helicity as a tornado forecast parameter. Preprints 16th Conference on Severe Local Storms, Banff, Amer. Meteor. Soc., 588-592.

Hart, J. A., and J. Korotky, 1991: The SHARP Workstation v1.50. WSFO Charleston, National Weather Service, NOAA, U.S. Department of Commerce, 62 pp.

Kelly, D. L., J. T. Schaefer, R. P. McNulty, C. A. Doswell III, and R. F. Abbey, Jr., 1978: An augmented tornado climatology. Mon. Wea. Rev., 106, 1172-1183.

Kitzmiller, D. H., W. E. McGovern, and R. E. Saffle, 1992: The NEXRAD severe weather potential algorithm. NOAA Technical Memorandum NWS TDL 81, National Oceanic and Atmospheric Administration, U.S. Department of Commerce, 76 pp. [NTIS PB92197102]

Lilly, D. K., 1986: The structure, energetics, and propagation of rotating convective storms. Part II: Helicity and storm stabilization. J. Atmos. Sci., 43, 126-140.

Maddox, R. A., 1976: An evaluation of tornado proximity wind and stability data. Mon. Wea. Rev., 104, 133-142.

McDonald, M., and R. E. Saffle, 1989: RADAP-II archive data user's guide. TDL Office Note 89-2, National Weather Service, NOAA, U.S. Department of Commerce, 16 pp.

Miller, R. C., 1972: Notes on analysis and severe-storm forecasting procedures of the Air Force Global Weather Central. Technical Report 200 (Rev.), Air Weather Service, U.S. Air Force, 190 pp.

Woodall, G. R., 1990: Qualitative analysis and forecasting of tornadic activity using storm-relative environmental helicity. NOAA Technical Memorandum NWS SR-127, National Oceanic and Atmospheric Administration, U.S. Department of Commerce, 57 pp.